Comptes Rendus

Géoscience

Sciences de la Planète

Laurent Jeanneau, Emilie Jardé, Justine Louis, Alexandrine Pannard, Marine Liotaud, Françoise Andrieux-Loyer, Gérard Gruau, Florian Caradec, Emilie Rabiller, Nathalie Lebris and Anniet Laverman

How the origin of sedimentary organic matter impacts the benthic nutrient fluxes in shallow coastal mudflats

Research article — Biogeochemistry

How the origin of sedimentary organic matter impacts the benthic nutrient fluxes in shallow coastal mudflats

Laurent Jeanneau [*, a], **Emilie Jardé** [a], **Justine Louis** [b, c], **Alexandrine Pannard** [b], **Marine Liotaud** [a], **Françoise Andrieux-Loyer** [c], **Gérard Gruau** [a], **Florian Caradec** [c], **Emilie Rabiller** [c], **Nathalie Lebris** [b] and **Anniet Laverman** [b]

[a] Univ Rennes, CNRS, Géosciences Rennes, UMR 6118, F-35000 Rennes, France

[b] Univ Rennes, CNRS, ECOBIO, UMR 6553, F-35000 Rennes, France

[c] Ifremer, DYNECO, F-29280 Plouzané, France

E-mails: laurent.jeanneau@univ-rennes1.fr (L. Jeanneau),
emilie.jarde@univ-rennes1.fr (E. Jardé), justine.louis@ceva.fr (J. Louis),
alexandrine.pannard@univ-rennes1.fr (A. Pannard), marine.liotaud@univ-rennes1.fr
(M. Liotaud), Francoise.Andrieux@ifremer.fr (F. Andrieux-Loyer),
gerard.gruau@univ-rennes1.fr (G. Gruau), Florian.Caradec@ifremer.fr (F. Caradec),
Emilie.Rabiller@ifremer.fr (E. Rabiller), nathalie.lebris@univ-rennes1.fr (N. Lebris),
anniet.laverman@univ-rennes1.fr (A. Laverman)

Abstract. The origin of sedimentary organic matter (SOM) has often been mentioned as a driver of SOM reactivity. This was quantified by statistically relating the isotopic and lipid composition of SOM to benthic nutrient fluxes in 200 intertidal mudflats sampled along the Brittany coast (France). The origin of SOM explained 24% and 31% of the variance of NH_4^+ and PO_4^{3-} fluxes, respectively. The NH_4^+ fluxes were driven by the uptake by phytoplankton of dissolved anthropogenic N exported from agricultural catchments. Their sedimentation is favoured by low hydrodynamic conditions, enriching the sediments with labile OM. The PO_4^{3-} fluxes were driven by the sedimentation of particulate P exported through agricultural soil erosion.

1. Introduction

Benthic nutrient fluxes in coastal ecosystems, especially in shallow environments, are impacted by both biotic and abiotic processes in the sediment [Boynton et al., 2018, Santschi et al., 1990, Ståhlberg et al., 2006]. One of the major processes of the early diagenesis of sediment is the microbial degradation of sedimentary organic matter (SOM), producing ammonium (NH_4^+) and phosphate (PO_4^{3-}) and the consequent fluxes of N and P at the sediment–water interface [Flint and Kamykowski, 1984, Sigmon and Cahoon, 1997, Anderson et al., 2003].

* Corresponding author.

The degradation of SOM, and consequently N and P fluxes, depends on its quantity and composition but also on external factors such as physico-chemical characteristics of the sediments (porosity, grain-size and mineralogy), temperature and availability of electron acceptors as well as microbial and macrobenthic activities and diversities [Arndt et al., 2013, Freitas et al., 2021, LaRowe et al., 2020]. However, the relative significance of these factors remains poorly quantified however [Freitas et al., 2021], preventing the prediction of the effect of climate and environmental changes as well as the development of mitigation strategies.

Although the amount of SOM has been reported as an important driver of mineralization activity in coastal areas [Sloth et al., 1995, Mesnage et al., 2007], the composition of SOM has also been shown to play a key role in benthic nutrient cycling [Andrieux-Loyer et al., 2014, Albert et al., 2021]. The composition of SOM in coastal areas is tightly linked to its origin and is the result of a large diversity of allochthonous and autochthonous primary producers (such as phytoplankton, benthic macroalgae, microphytobenthos, seagrasses andwoody plants), as well as anthropogenic OM [Bianchi and Bauer, 2011, and references therein]. Among natural sources of OM, the pathways from sources to sediments and the probability of early biodegradation differ greatly between autochthonous and allochthonous OM. Allochtonous OM has undergone transport from sources to sediments and along its transfer has possibly been subject to biodegradation and can be protected by interactions with mineral surfaces, in contrast to autochthonous OM which only experiences vertical transport and settling. Consequently, the latter would be richer in labile molecules, which could explain the higher reactivity in sediments following phytoplanktonic blooms [Franzo et al., 2019, Grenz et al., 2000]. Moreover, anthropogenic sources of OM from sewage and soil fertilization by agricultural amendments may also drive sedimentary P cycling [Ait Ballagh et al., 2020, Khalil et al., 2018]. However, the respective role of allochtonous versus autochthonous and anthropogenic versus natural OM on the biodegradability of SOM and the diffusive and advective benthic nutrient fluxes remains unclear.

In order to investigate the relationships between the origin of SOM and benthic nutrient fluxes, 200 intertidal mudflat sediments from 12 mudflats along the coastline of Brittany, France were sampled. In this region, marine intertidal mudflats are influenced by river discharges and large tidal fluctuations. Agricultural intensification and the urbanization of watersheds have led to coastal eutrophication, where macroalgal "green tides" occur regularly in spring [Ménesguen et al., 2019, Perrot et al., 2014, Schreyers et al., 2021]. Designing the investigation at the scale of the region allows the investigation of variations in the proportions of natural (marine versus terrestrial) and anthropogenic sources of SOM, while terrestrial plant precursors, land use and sources of anthropogenic pressure remain unchanged. The composition of SOM was studied by a combination of isotopic (δ^{13}C and δ^{15}N values) and lipid (aliphatic hydrocarbons (*n*-alkanes and hopanes), sterols and stanols, fatty acids, fatty alcohols, and aromatic hydrocarbons including polycyclic aromatic hydrocarbons-PAH) analyses classically used to investigate the sources of SOM [Freese et al., 2008, Volkman et al., 2000]. The ability of sediments to release NH_4^+ and PO_4^{3-} fluxes through diffusion were determined using incubations with intact sediment cores under the same ambient experimental conditions (dark, controlled temperature, artificial overlying water) [Louis et al., 2021]. Finally such a dataset allows the use of canonical redundancy analysis (RDA) and variance partitioning in order to explain the spatial variability of the NH_4^+ and PO_4^{3-} fluxes as independent parameters related to (i) the variation of the SOM origin (elemental and isotopic ratios, lipid markers) and (ii) the variation of the elemental composition (N, P, C) and physical properties (grain size, porosity) of the sediment [from Louis et al., 2021].

The different analytical techniques will shed light on the composition of the SOM, which will allow the determination of its spatial variability and origin. In combination with statistical analysis this will allow relating quantitatively the impact of the origin of SOM on benthic nutrient fluxes in shallow coastal environments.

2. Materials and methods

2.1. *Study sites and sampling*

All of the study sites were macrotidal mudflats, located in Brittany, north-western France, and have been described in detail previously [Louis et al.,

2021]. In short, 200 sediment samples were collected at low tide at 45 sites and were classified into 12 mudflats (Figure 1) during spring 2019. Sampling sites were divided into three classes: bay, lower estuary and middle estuary according to their distance to the mouth; from 0 to 5 km and from 5 to 15 km, respectively. Sediment cores (10 cm depth) were sampled with PVC tubes (diameter = 6 cm, h = 20 cm) to measure the nutrient benthic fluxes, and another tube (diameter = 9 cm, h = 5 cm) was sampled to characterize the SOM (elemental, isotopic and lipid composition) and physico-chemical parameters (grain size distribution and porosity) in the upper 5 cm layer. Even though the flux measurements were carried out with 10 cm depth sediments, the nutrient fluxes are the result of gradients over the first 2 to 5 cm [Lee and Kim, 1990, Akbarzadeh et al., 2018]. In order to capture this reactive zone, the first five cm of the sediment were analyzed for physico-chemical parameters. Elemental composition (total organic C, total N, total, organic and iron oxide bound P), grain-size distribution, porosity and benthic nutrients fluxes were described in a previous paper [Louis et al., 2021], while isotopic and lipid compositions are the new data discussed in this paper.

2.2. *Isotopic analysis*

The carbon and nitrogen isotopic compositions (δ^{13}C and δ^{15}N values) were determined using an element analyzer (FLASH™ EA 2000 IRMS) coupled with an isotopic ratio mass spectrometer (DELTA V™ plus). An aliquot of the 5 cm pooled sample was freeze-dried, crushed and acid-treated with 2N HCl to remove the carbonate and was subsequently rinsed with deionized water. After centrifugation, the carbonate-free sample was dried at 60 °C, and ground before being placed into a tin capsule for stable C isotopic analysis. A second aliquot without an acidification treatment was used for the total nitrogen in bulk OM (TN) and stable N isotopic analysis. All isotopic analyses were performed once and data were expressed in the conventional delta notation relative to the Vienna Pee Dee Belemnite for δ^{13}C values and to atmospheric N_2 for δ^{15}N values. Data calibration and determination of the accuracy and reproducibility was carried out using two international standards IAEA-N2 and IAEA-CH-6 and a certified standard IVA33802151 organic-rich sediment.

Repeated analysis indicated analytical uncertainty better than ±0.2‰.

2.3. *Lipid marker analysis*

An aliquot of the 5 cm pooled sample was freeze-dried and crushed. Approximately 30 g of this sample was extracted with approximately 100 mL of dichloromethane using an accelerated solvent extractor (Dionex™ASE™ 200) as per the following conditions, modified from Derrien et al. [2011]: 33 mL cells, 5 min heating at 100 °C and 60 bars, 10 min static phase, completed with 80% flush and 20-s purge with nitrogen. Elemental sulfur was removed from the total lipid fraction by reduction on metallic copper. After evaporation of DCM under a gentle stream of nitrogen, the total lipid extract was fractionated into aliphatic hydrocarbons, aromatic hydrocarbons and polar compounds on a silica column by successive elution with cyclohexane, cyclohexane/dichloromethane (2/1, v/v) and methanol/dichloromethane (1/1, v/v). Polar fractions were analyzed by capillary gas chromatograph-mass spectrometer (QP2010SE GC-MS, Shimadzu) after derivatization using a mixture of N,O-bis(trimethylsilyl) trifuoroacetamide (BSTFA) and trimethylchlorosilane (TMSC) (99/1, v/v), whereas the aliphatic and aromatic fractions were analyzed without further treatment. The injector used was in splitless mode and maintained at a temperature of 310 °C. The chromatographic separation of the three lipid fractions was performed on a SLB-5MS capillary column (length = 60 m, diameter = 0.25 mm, film thickness = 0.25 μm) under the following temperature conditions: 70 °C (held for 1 min) to 130 °C at 15 °C/min, the 130 °C to 300 °C (held for 15 min) at 3 °C/min. The helium flow was maintained at 1 ml/min. The chromatograph was coupled to the mass spectrometer by a transfer line heated at 280 °C. The ionization was performed by electronic impact and analyses were performed in full scan mode. The organic compounds were quantified by using an external calibration adding internal standards in the solutions containing the aliphatic hydrocarbons (internal standards: nC$_{20}$D$_{42}$; nC$_{24}$D$_{50}$; nC$_{30}$D$_{62}$; α-cholestane), aromatic hydrocarbons (internal standards: Naphthalene-D8; Acenaphtene-D10; Phenanthrene-D10; Chrysene-D12; Perylene-D12) and polar compounds (internal standards:
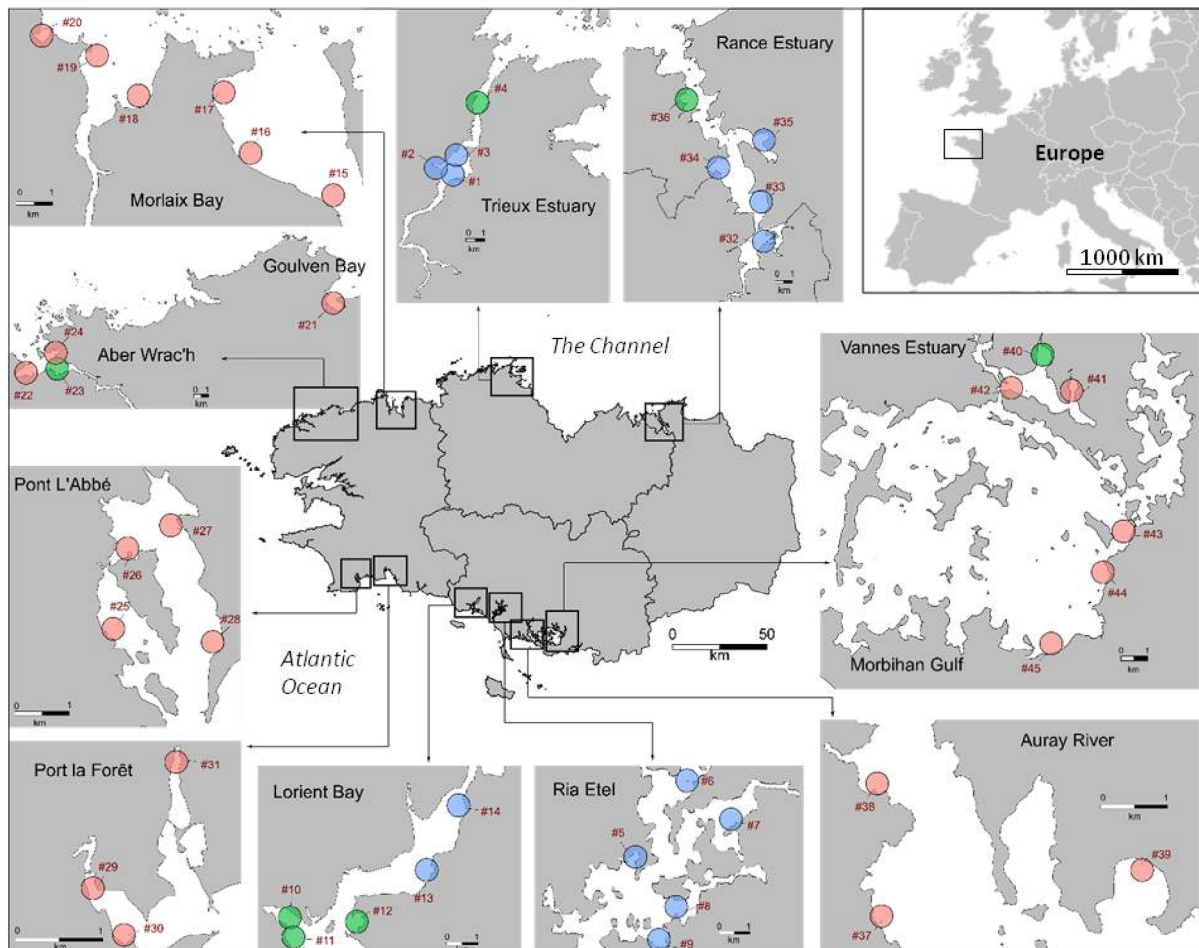
Figure 1. Location of the mudflats and sampling sites ($n = 45$) on the Brittany coast. Goulven Bay and Aber Wrac'h are two different mudflats, as are Vannes Estuary and Morbihan Gulf. The sampling sites were divided into three groups according to their geographic locations into "Bay" (pink), "Lower estuary" (green) and "Middle estuary" (blue).

$n\text{C}_{20}\text{D}_{42}$; $n\text{C}_{24}\text{D}_{50}$; $n\text{C}_{30}\text{D}_{62}$; α-cholestane) as per Jeanneau et al. [2008].

These analyses provided the total concentration of lipid markers in the dry mass sediment. The results were also expressed as the proportion of each lipid marker as a function of the sum of all lipid compounds quantified in the sediment. Unless otherwise stated, results are presented as the average $\pm$ the standard deviation.

2.4. *Benthic nutrient fluxes*

The NH_4^+ and PO_4^{3-} fluxes are previous results described in detail in Louis et al. [2021]. Briefly, intact

sediment cores were incubated in the dark for 4 h directly on site in a mobile laboratory under controlled temperature within one hour of sampling. The overlying water was replaced by 150 mL nutrient-free artificial seawater and gently aerated and stirred by bubbling in order to preserve the oxic conditions in the overlying water and to prevent the build-up of concentration gradients at the sediment–water column interface. The core incubations were conducted under controlled temperature in the dark and by using nutrient-free artificial seawater as the overlying water in order to exclude these environmental variables (temperature and light) related to benthic NH_4^+ and PO_4^{3-} fluxes and focusing on the relation with the

sedimentary characteristics. These standardized core incubations allowed to assess benthic fluxes mimicking the mudflat submerged during high tide by the oxygenated coastal water and are thus potential benthic fluxes, throughout the manuscript indicated as "benthic fluxes". Water samples were collected in the overlying water after 2 h and 4 h of incubation, filtered (0.22 μm) and stored at 4 °C for less than 3 days until nutrient analysis. The NH_4^+ and PO_4^{3-} fluxes ($μmol·m^{-2}·h^{-1}$) across the sediment–water interface were estimated by using the change in the molar concentration of the solute in the known volume of overlying water as a function of incubation time and the surface area of the sediment core. If the rate of nutrient release from the sediment did not follow a linear trend over the incubation period, only the sample at 2 h was considered in the flux estimation. Fluxes have already been described in Louis et al. [2021]. The data are given in Supplementary Table S1.

2.5. *Data analysis*

2.5.1. *Classification of lipid markers for the investigation of SOM sources*

A total of 180 compounds from five chemical classes (sterols and stanols, fatty acids, fatty alcohols, aliphatic hydrocarbons and aromatic hydrocarbons) were identified in the sediment samples and were classified according to the literature (Table 1) and diagnostic ratios (Table 2) into eleven categories: ten sources (microbial matter, terrestrial plants, phytoplankton, green macroalgae, pelagic and benthic microalgae, algal matter, macrophytes, fecal matter, crude oil and petroleum by-products, combustion products) and one for ubiquist compounds that can derive from multiple sources. For the categories "Microbial matter", "Terrestrial plants", "Crude oil or petroleum by-products" and "Combustion products", the compounds were classified according to their functional groups as well as the correlations among them established by a Principal Component Analysis (PCA) finally resulting in 16 lipid marker groups (Table 1). The PCA analysis was performed using the R-studio software with the "FactoMineR" package.

2.5.2. *Statistical analyses*

The differences were investigated by student *t*-test, unless otherwise specified, and are mentioned in the text for *p*-values < 0.05.

2.5.3. *Canonical redundancy analysis (RDA) and variance partitioning*

The RDA allows determining linear relationships between responses (matrix *Y*) and explanatory (matrix *X*) variables. In the present study, the authors aimed to explain the benthic nutrient fluxes (response variables) by the sedimentary parameters (explanatory variables). To explain the spatial variability in the NH_4^+ and PO_4^{3-} fluxes (response variables), two constrained analyses were carried out in parallel. For the first analysis, explanatory variables were qualitative parameters related to SOM sources (elemental ratios, isotopic compositions and the proportions of lipid marker groups), hereafter called "SOM origin". Explanatory variables for the second analysis were previously published in Louis et al. [2021]. They were quantitative parameters related to the sediment composition (the contents of TN, TOC, iron oxide-bound P (Fe-P) and organic P (Org-P)) and the microbial access to SOM (percentage of mud and porosity), hereafter called the "physico-chemical composition". A Canonical Redundancy Analysis (RDA) was chosen in both cases, assuming a linear relationship between the response and explanatory variables. This dissymmetrical analysis combines the concepts of ordination and regression, with explanatory variables used to recalculate the response variables. The new canonical axes are thus a linear combination of the initial explanatory variables. The best explanatory variables in each matrix were selected by the "ordistep" function of the "vegan" package [R software; Borcard et al., 2018, Oksanen et al., 2013] based on the Akaike Information Criterion (AIC) through automatic permutation tests of the ordination model and forward model selection. The non-collinearity between the selected variables was then checked with the Variance Inflation Factor (VIF) (a threshold value was set at 10).

In order to determine the linear relationships between all of the previously selected variables and the benthic nutrient fluxes, an RDA was performed and tested by the permutation test.

With the selected explanatory variables, variance partitioning was then used to quantify the variance proportion of the NH_4^+ and PO_4^{3-} fluxes independently explained by both the "SOM origin" and "physico-chemical composition" parameters

Table 1. Classification of identified lipid markers in term of chemical classes, sources and groups

Chemical classes	Compounds	Sources	Groups
Fatty acids	*iso* and *anteiso* nC$_{17:0}$[1,2]	Microbial matter	Bacteria 1
	iso and *anteiso* nC$_{15:0}$[1,2]	Microbial matter	Bacteria 2
	nC$_{20:0}$ to nC$_{30:0}$; ω-hydroxy acids nC$_{16}$ to nC$_{24}$; α, ω diacids nC$_{16}$ to nC$_{26}$[1,2]	Terrestrial plants	Plants 4
	nC$_{10:0}$ to nC$_{19:0}$; brC$_{12:0}$; brC$_{13:0}$; brC$_{14:0}$; brC$_{16:0}$; nC$_{16:1}$; nC$_{18:1}$; nC$_{20:1}$; nC$_{22:1}$; nC$_{18:2}$[1,2]	Ubiquist	
Fatty alcohols	nC$_{20:0}$ to nC$_{30:0}$[3]	Terrestrial plants	Plants 3
	nC$_{11:0}$ to nC$_{19:0}$[3]	Ubiquist	
Sterols and stanols	Coprostanol; Epicoprostanol; 24-Ethylcoprostanol; 24-Ethylepicoprostanol[4]	Fecal matter	Fecal
	Cholesta-5,22(E)dien-3β-ol; Brassicasterol[5,6]	Phytoplankton	Phytoplankton
	Campesterol; Stigmasterol[7]	Terrestrial plants	Plants 2
	Fucosterol; Isofucosterol[8]	Green macroalgae	Green macroalgae
	Cholesterol; Sitosterol; 5α-Cholestan-3-one; Cholestanol; Epicholestanol; Campestanol; Sitostanol[6]	Ubiquist	
Aliphatic hydrocarbons	nC$_{11}$ to nC$_{14}$ n-alkanes; Bicyclohexane[9,10]	Crude oil or petroleum by-products	Petroleum by-product 1
	nC$_{15}$ to nC$_{19}$ n-alkanes[7,11]	Pelagic and benthic microalgae	Microalgae
	nC$_{20}$ to nC$_{26}$ n-alkanes with an odd over even predominance (CPI > 2)[11,12,13]	Macrophytes	Macrophytes
	nC$_{20}$ to nC$_{26}$ n-alkanes without an odd over even predominance (CPI ~ 1); nC$_{26}$ to nC$_{35}$ n-alkanes without an odd over even predominance (CPI ~ 1); Tricyclic and pentacyclic triterpanes (hopanes)[10]	Crude oil or petroleum by-products	Petroleum by-product 2
	nC$_{26}$ to nC$_{35}$ n-alkanes with an odd over even predominance (CPI > 5)[3,14]	Terrestrial plants	Plants 1
	Neophytadiene (3 isomers)[15,16]	Algal matter	Algae
Aromatic hydrocarbons	Phenanthrene; Anthracene; methyl-, dimethyl- and trimethyl-phenanthrene and -anthracene; Fluoranthene; Pyrene methyl-and dimethyl-fluoranthene and -pyrene[17]	Combustion products	Combustion 1
	Benzonaphthothiophene; Benzo(a)anthracene; Chrysene; methyl-and dimethyl-benzo(a)anthracene and -chrysene; Benzofluoranthene; Benzopyrene; methyl-benzofluoranthene and -benzopyrene; Perylene; Dibenzo(a,h)anthracene; Indeno[1,2,3-cd]pyrene; Benzo(g,h,i)perylene[17]	Combustion products	Combustion 2

(1) Derrien et al. [2017]; (2) Meziane and Tsuchiya [2000]; (3) Eglinton and Hamilton [1967]; (4) Leeming et al. [1996]; (5) Cook et al. [2004]; (6) Volkman [1986]; (7) Brassel et al. [1978]; (8) Iatrides et al. [1983]; (9) Woolfenden et al. [2011]; (10) Peters and Moldovan [1993]; (11) Jaffé et al. [2001]; (12) Chevalier et al. [2015]; (13) Ficken et al. [2000]; (14) Bray and Evans [1961]; (15) López-Rosales et al. [2019]; (16) Santos et al. [2015]; (17) Yunker et al. [2002].

[Borcard et al., 1992]. Therefore, a comparison between the effects of the SOM origin on benthic nutrient fluxes with those of other known sedimentary characteristics was established. The significance of each fraction of interest was tested by the permutation test.

The "rda", "vif.cca", "anoca.cca" and "varpart" functions of the "vegan" package (R software) were

Table 2. Diagnostic ratios calculated on the distributions of *n*-alkanes and PAHs

Ratio	Formula	Values	Sources
n-Alkanes			
CPI[1]	$\dfrac{1}{2}\left(\dfrac{\sum n\mathrm{C}_{25,27,29,31,33,35}}{\sum n\mathrm{C}_{24,26,28,30,32}} + \dfrac{\sum n\mathrm{C}_{25,27,29,31,33,35}}{\sum n\mathrm{C}_{24,26,28,30,32,34}}\right)$	~1	Petrogenic OM
		>5	Terrestrial plants
TAR[2]	$\dfrac{\sum n\mathrm{C}_{25,27,29,31}}{\sum n\mathrm{C}_{15,17,19}}$	<1	Aquatic OM
		>5	Terrestrial OM
Paq[3]	$\dfrac{\sum n\mathrm{C}_{23,25}}{\sum n\mathrm{C}_{23,25,29,31}}$	<0.25	Terrestrial plants
		0.4–0.6	Emerged aquatic plants
		>0.6	Submerged aquatic plants
PAHs			
R1[4]	$\dfrac{Benzo(a)anthracene}{Benzo(a)anthracene + Chrysene}$	<0.2	Petrogenic OM
		0.2–0.35	Mixed sources
		>0.35	Combustion
R2[5]	$\dfrac{Benzo(a)pyrene}{Benzo(a)pyrene + Benzo(e)pyrene}$	~0.5	Freshly emitted road particles
		<0.5	Aged road particles
R3[6]	$\dfrac{Retene}{Retene + Chrysene}$	~1	Wood combustion
R4[4]	$\dfrac{Indeno[1,2,3-cd]pyrene}{Indeno[1,2,3-cd]pyrene + Benzo(ghi)perylene}$	<0.2	Petrogenic OM
		0.2–0.5	Combustion of petrogenic OM
		>0.5	Combustion of recent OM and coal
R5[7]	$\dfrac{Benzo(a)pyrene}{Benzo(ghi)perylene}$	<0.6	Non traffic related sources
		>0.6	Traffic related sources

(1) Bray and Evans [1961]; (2) Ortiz et al. [2013]; (3) Ficken et al. [2000]; (4) Yunker et al. [2002]; (5) Oliveira et al. [2011]; (6) Yan et al. [2005]; (7) Katsoyiannis et al. [2007].

used to perform the RDA analysis, VIF calculation, permutation test and variance partitioning, respectively. The "dist.dudi" function of the "ade4" package and the "hclust" function (R software) were used to perform the hierarchical cluster analysis. The data were previously standardized with the "scale" function prior to the multivariate analysis.

3. Results

3.1. *Benthic nutrient fluxes*

These data are described in details in Louis et al. [2021]. This section summarized the main results that are presented in Figure 2. The average of the NH_4^+ fluxes was 101 ± 117 µmol·m^{-2}·h^{-1}. A large spatial variability of NH_4^+ fluxes was observed at both the regional and local (mudflat) scale. As an example, large differences were observed within the Vannes Estuary with 410 ± 58 µmol·m^{-2}·h^{-1} for the sampling site #41 and only 12 ± 12 µmol·m^{-2}·h^{-1} for the site #42. The PO_4^{3-} fluxes were generally 20-fold lower than the NH_4^+ fluxes, with an average flux of 17 ± 20 µmol·m^{-2}·h^{-1} (Figure 2). High PO_4^{3-} fluxes were observed for the sites located in the Lorient Bay (e.g. site #13, mean = 51 ± 7 µmol·m^{-2}·h^{-1}), Pont L'Abbé (e.g. site #28, mean = $66 + 71$ µmol·m^{-2}·h^{-1})
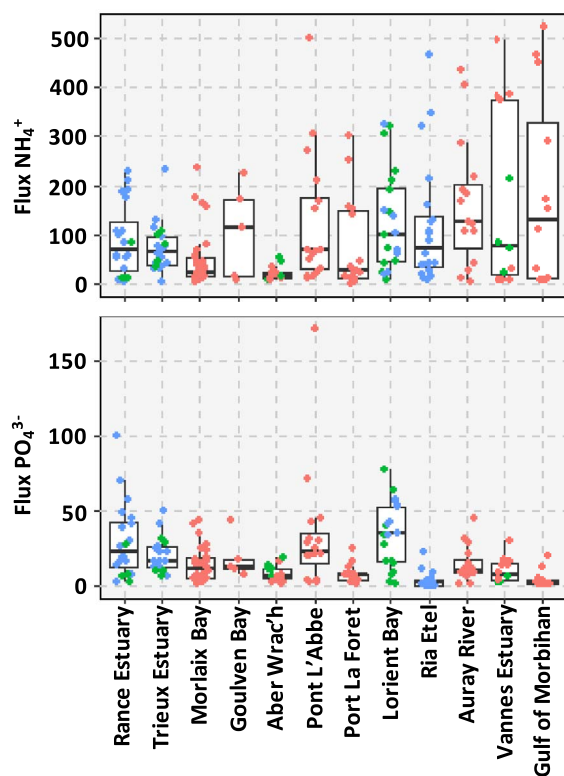
Figure 2. Boxplot of the benthic (a) NH_4^+ and (b) PO_4^{3-} fluxes ($\mu mol \cdot m^{-2} \cdot h^{-1}$) at the sediment–water interface displayed by mud-flat. The color of the dots differentiates the ecosystems between middle estuaries (blue), lower estuaries (green) and bays (pink).

and along the Rance Estuary (e.g. site #33, mean = $54 + 42 \ \mu mol \cdot m^{-2} \cdot h^{-1}$).

3.2. *SOM characterization via isotopic and lipid analysis*

3.2.1. *Isotopic compositions*

The $\delta^{13}C$ values varied from -24.3 to $-16.2‰$, with the highest values measured in the Gulf of Morbihan (mean value = $-17.0 \pm 0.6‰$, sites #43, #44 and #45). Lower values of $\delta^{13}C$ ($<-22‰$) corresponded to sediments collected in the upstream sites of Lorient Bay (sites #13 and #14, mean values = $-23.0 \pm 0.4‰$ and $-23.4 \pm 1.7‰$), the Trieux Estuary (sites #1 and #2, mean values = $-22.9 \pm 0.3‰$ and $-23.6 \pm 0.5‰$), and Port la Forêt (site #31,

mean value = $22.6 \pm 0.5‰$) (Figure 3). The $\delta^{15}N$ values varied from 5.8 to 10.5‰. Highest values of $\delta^{15}N$ were measured in the Vannes Estuary (site #41, mean value = $9.5 \pm 0.7‰$), as well as in the Rance Estuary (mean value = $8.4 \pm 0.4‰$). The lowest values of $\delta^{15}N$ were measured in the bay of Aber Wrac'h (site #22, mean value = $6.1 \pm 0.3‰$). In general, the sediments from middle estuaries were characterized by the highest values of $\delta^{15}N$ and the lowest values of $\delta^{13}C$ and the opposite was observed for the sediments sampled in the bays (Figure 3).

3.2.2. *Distribution and sources of lipids*

Considering all the samples, the relative proportion of the five investigated chemical classes is dominated by sterols and stanols (Figure 4). They represent $30 \pm 12\%$ (mean $\pm$ sd) of the investigated compounds. Fatty acids (FA) and aliphatic hydrocarbons (especially *n*-alkanes) represented similar proportions of the investigated compounds followed by fatty alcohols. Aromatic hydrocarbons occurred in low proportions in these sediments, representing $2 \pm 4\%$ of the investigated compounds.

The distribution of the 17 sterol and stanol compounds were dominated by cholesterol ($31 \pm 9\%$ of sterol and stanol proportions) and sitosterol ($20 \pm 6\%$). Source specific sterols and stanols represented $12 \pm 2\%$, $9 \pm 3\%$, $6 \pm 2\%$ and $4 \pm 3\%$ for terrestrial plants, phytoplankton [Volkman, 1986, Cook et al., 2004], fecal matter [Leeming et al., 1996] and green macroalgae [Iatrides et al., 1983], respectively. This chemical class was composed of $70 \pm 5\%$ of ubiquist compounds. The spatial variability of the distribution of the 4 fecal stanols (coprostanol, epicoprostanol, 24-ethylcoprostanol and 24-ethylepicoprostanol) was investigated by a statistical treatment modified from Derrien et al. [2011], Derrien et al. [2012] and Jardé et al. [2018]. This statistical treatment allows the determination of the proportion of the three main fecal matter sources in Brittany (pig slurry, cow manure and waste water treatment plant effluents) into the fecal stanol distribution [Jardé et al., 2018] (Figure S1). The distribution of fecal stanols in the samples resulted mainly from cow manure ($68 \pm 14\%$) and pig slurry ($11 \pm 15\%$) exports and inputs from waste water treatment plant (WWTP) effluent or non-connected installations ($21 \pm 8\%$).

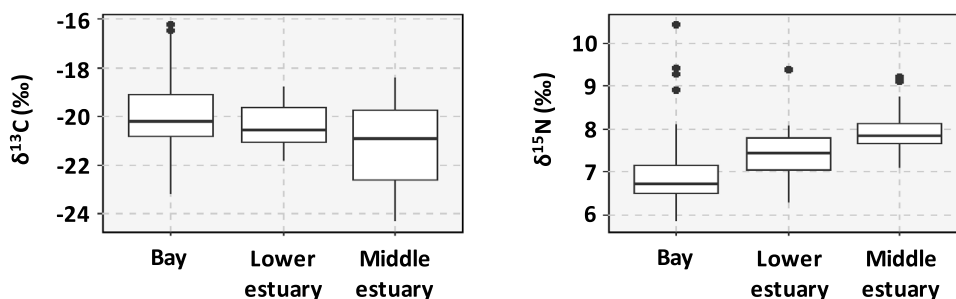The second most important chemical class in terms of proportion are fatty acid compounds. Fatty

Figure 3. Ranges of variation of the isotopic ratios $\delta^{13}C$ and $\delta^{15}N$ as a function of the type of environment.
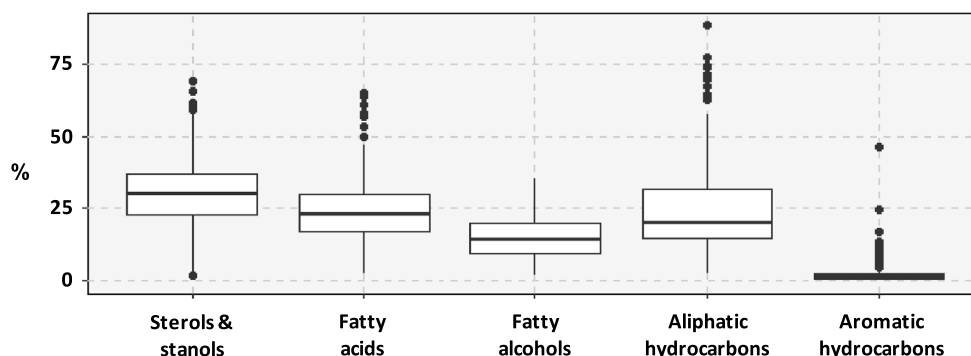

Figure 4. Ranges of variation of the proportion of the investigated chemical classes among identified compounds.

acids (FAc) represented $25 \pm 11\%$ among the investigated compounds (Figure 4). Their distribution was dominated by nC$_{16:0}$ that represented $24 \pm 4\%$ of FAc. Due to their occurrence in both bacteria and algae [Cranwell et al., 1987, Meziane and Tsuchiya, 2000], low molecular weight (LMW) FAc from nC$_{10:0}$ to nC$_{19:0}$ were classified as ubiquist, with the exception of *iso* and *anteiso* C$_{15:0}$ and C$_{17:0}$ that are specific of bacteria. Ubiquist and bacterial FAc represented $66 \pm 12\%$ and $5 \pm 2\%$ of FAc, respectively. The apparent low proportion of bacterial FAc is due to the fact that a large portion of the LMW FAc was classified as ubiquist. High molecular weight (HMW) FAc from nC$_{20:0}$ to nC$_{30:0}$, ω-hydroxy FAc and α, ω diacids originated from terrestrial plants [Eglinton and Hamilton, 1967], representing $29 \pm 8\%$ of the FAc.

Fatty alcohols (FAl) represented $15 \pm 7\%$ of the investigated compounds (Figure 4). Their distribution was dominated by nC$_{24}$, nC$_{26}$ and nC$_{28}$ that represented $15 \pm 5\%$, $26 \pm 6\%$ and $16 \pm 5\%$ of FAl, respectively. HMW FAl from nC$_{20}$ to nC$_{30}$ with a predom-

inance of molecules with an even number of carbon are characteristic of terrestrial plants [Cranwell et al., 1987], representing $86 \pm 9\%$ of FAl. The remaining (FAl from nC$_{11}$ to nC$_{19}$) were classified as ubiquist due to their occurrence in both bacteria and algae [Cranwell, 1974].

The chemical class of aliphatic hydrocarbons represented $26 \pm 18\%$ of the investigated compounds and was dominated by n-alkanes ($94 \pm 5\%$) (Figure 4). This chemical class exhibits the most variable distribution as highlighted by the mean relative standard deviation that is significantly higher for n-alkanes than for the other chemical classes (Wilcoxon test, $p < 0.001$). The main compounds of this distribution were nC$_{13}$ ($16 \pm 14\%$) and nC$_{29}$ ($12 \pm 6\%$). The carbon preference index (CPI) ranged from 1.7 to 8.6 with a mean value of 5.0 ± 1.4 (Table 2; Figure 5a). This range highlights that the proportion of crude oil and/or petroleum byproducts in the aliphatic fingerprint changed from a low proportion for CPI > 5 to a high proportion for CPI close to 1 [Bray and Evans, 1961]. The terrestrial to aquatic ratio (TAR) ranged from 0.9 to 39

with a mean value at 7.2 ± 5.4 (Figure 5b). Only two samples (#44 and #45 in the Gulf of Morbihan) exhibit TAR < 1 characteristic of *n*-alkanes coming mainly from marine sources [Bourbonniere and Meyers, 1996]. Out of the 200 samples, 114 have TAR > 5 characteristic of *n*-alkanes originating mainly from terrestrial sources. TAR values from 1 to 5 were deduced for 83 samples, indicating a combination of marine and terrestrial sources. Such variabilities indicate a combination of several sources of OM for this chemical class as highlighted by the different types of chromatograms (Figure 6). The first source (Figure 6a) was characterized by low CPI and the occurrence of a large hump (unresolved complex mixture, UCM) on the chromatogram. This source was also characterized by higher proportion of tricyclic and pentacyclic triterpanes with values of the 22S/(22S + 22R) homohopane that ranged from 0.41 and 0.62 with an average value at 0.53 ± 0.03. This highlights the input of crude oil and/or heavy petroleum by-products such as road asphalt or lubricant oils [Peters and Moldovan, 1993]. The second source (Figure 6b) was characterized by a monomodal distribution of LMW *n*-alkanes from $n\mathrm{C}_{11}$ to $n\mathrm{C}_{15}$ with $n\mathrm{C}_{13}$ as the maximum. This distribution is very similar to the fingerprint of the diesel described by Woolfenden et al. [2011]. The third source (Figure 6c) was characterized by the predominance of HMW *n*-alkanes ($>n\mathrm{C}_{20}$) with a large odd-over-even predominance resulting in CPI > 5 characteristic of the input of terrestrial plants for *n*-alkanes from $n\mathrm{C}_{25}$ to $n\mathrm{C}_{35}$ and of emergent aquatic plants from $n\mathrm{C}_{21}$ to $n\mathrm{C}_{25}$. The Paq ratio (Figure 5c) can be used as a balance between these two natural sources [Ficken et al., 2000]. For 109 samples, the proportion of HMW *n*-alkanes was higher than 50% of *n*-alkanes and the CPI was higher than 3, indicating that the distribution of *n*-alkanes was dominated by natural inputs. For these samples, Paq ranged from 0.13 to 0.39 (average value of 0.26 ± 0.06). For Paq < 0.25 (43 samples), the HMW *n*-alkanes were inherited from only terrestrial plants. The remaining samples (66 samples) are characterized by a combination of terrestrial and emergent aquatic plants (0.25 < Paq < 0.4), which proportions have been determined using an end member mixing approach with 0.25 for terrestrial plants and 0.4 for emergent aquatic plants. The proportion of HMW *n*-alkanes coming from terrestrial plants in these 66 samples was $65 \pm 23\%$ (mean ± SD).

Aromatic hydrocarbons including polycyclic aromatic hydrocarbons (PAHs) represented $2 \pm 4\%$ (mean ± sd) of the investigated compounds. This proportion ranged from 0.1 to 47% but is below 5% for the majority (90%) of the samples. Two sites are characterized by high proportion of aromatic hydrocarbons, one in Ria d'Etel ($22 \pm 18\%$, site #5) and the other in Auray River ($10 \pm 5\%$, site #37). Among this chemical class, the 16 PAHs listed by the US Environmental Protection Agency (EPA) are often quantified in sediments as a measure of the anthropogenic pressure (Figure S2). Their sum was 425 ± 655 ng/g and ranged from 21 to 7489 ng/g of dry sediment. The distribution of PAHs depends on the sources of burned OM and can be used for their identification. The predominance of non methylated PAHs that represented $78 \pm 4\%$ (mean ± sd) of PAHs highlighted that they were mainly pyrogenic [Yunker et al., 2002]. Isomeric ratios calculated on PAH allow determining the main pyrogenic source (Table 2; Figure S3). The R4 ratio indicates a combination of pyrogenic OM coming from the combustion of petroleum and modern OM [Yunker et al., 2002]. The R3 ratio indicates a low contribution of wood burning [Yan et al., 2005], while the R1 and R5 ratios indicate emissions from road traffic as the main contributors of this pyrogenic OM [Katsoyiannis et al., 2007, Yunker et al., 2002]. Moreover the R2 ratio highlights that these particles have been aged by photolysis [Oliveira et al., 2011].

3.3. *Variance partitioning and canonical redundancy analysis*

Significant variables from the various datasets were selected to determine the relationship between biodegradability and OM sources while taking the sediment properties into account. The grain-size distribution, the porosity, the elemental composition of bulk OM and benthic nutrient fluxes were taken from Louis et al. [2021]. Benthic NH_4^+ and PO_4^{3-} fluxes are shown in Figure 6. In the "SOM origin" data matrix, the selected variables were $\delta^{13}\mathrm{C}$ values, $\delta^{15}\mathrm{N}$ values, and six lipid marker groups: "Fecal", "Petroleum products", "Microalgae", "Plants 3", "Plants 4" and "Bacteria 1" (see Table 1 for the composition of these groups). Regarding the "physicochemical composition" data matrix, the selected variables were the Fe-P, Org-P and the porosity. With
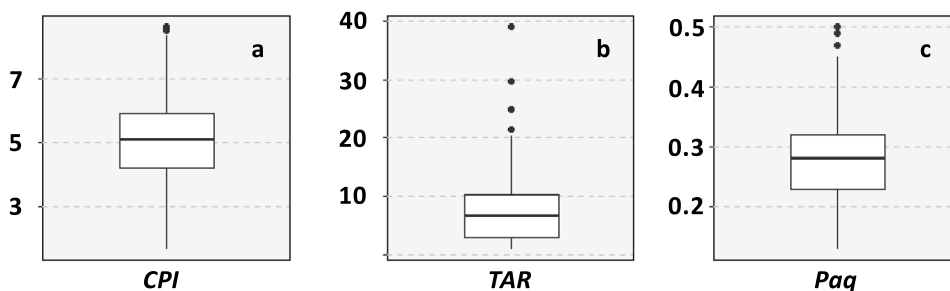
Figure 5. Ranges of variation of ratios calculated on the distribution of *n*-alkanes. The formulas and diagnostic values are given in Table 2.
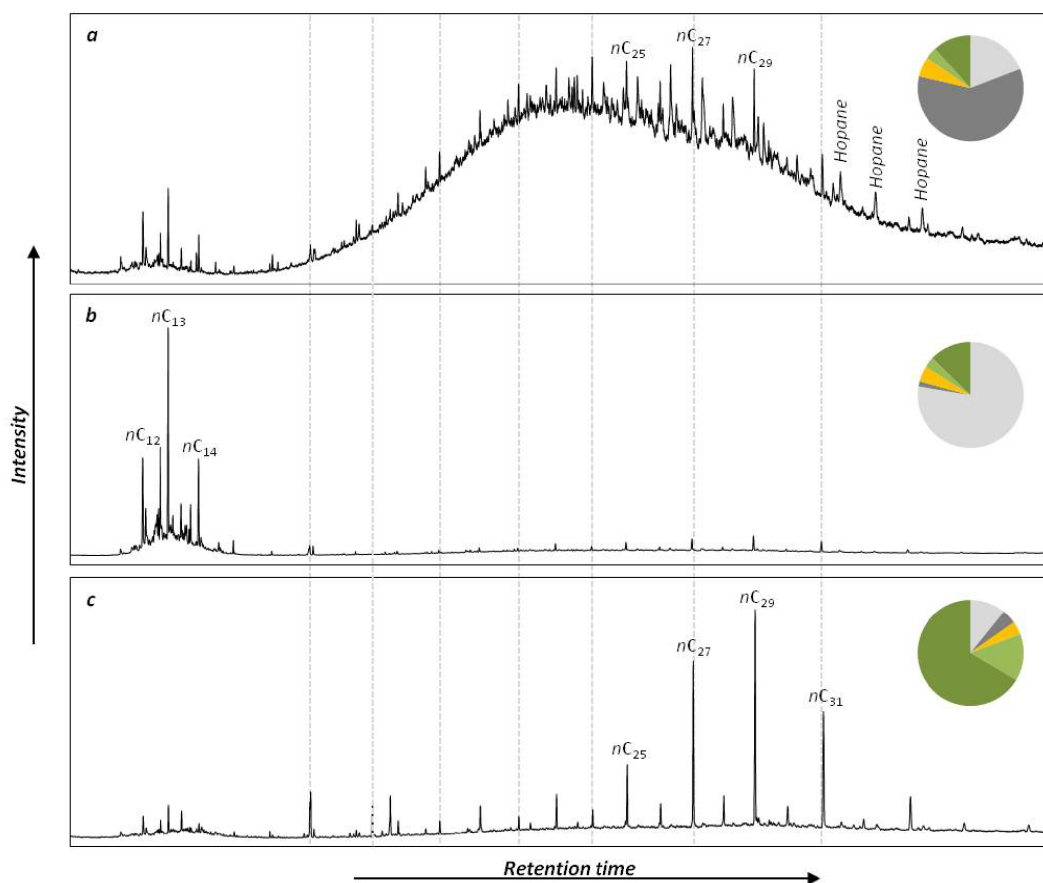

Figure 6. Typical chromatograms of aliphatic fractions from mudflats of Brittany: (a) crude oil dominated chromatogram from Morlaix Bay, site #18; (b) diesel dominated chromatogram from Vannes Estuary, site #40; (c) terrestrial plants dominated chromatogram from Trieux Estuary site #4. Pie charts represent the proportion of molecular markers from terrestrial plants (dark green), algae (light green), microalgae and bacteria (gold), diesel (light grey) and crude oil or heavy refined petroleum by-product (dark grey) in the aliphatic fraction.

these selected variables in both data matrices, the variance partitioning of the NH_4^+ and PO_4^{3-} fluxes was carried out and the results are presented in Figure 7. The selected "SOM origin" and "physico-chemical

composition" parameters explained 30 and 34% of the variance of the NH_4^+ and PO_4^{3-} fluxes respectively. The variables related to "SOM origin" significantly explained 16% of the variance of the NH_4^+ fluxes (F = 5.3, $p = 0.001$) and 16% of the variance of PO_4^{3-} fluxes (F = 5.8, $p = 0.001$), compared to 6 and 3% with the "physico-chemical composition" variables. The "SOM origin" and "physico-chemical composition" variables shared between 8 and 15% of the variance partitioning of the NH_4^+ and PO_4^{3-} fluxes, respectively.

In order to relate the benthic nutrient fluxes with the selected variables from the SOM origin, the isotopic composition and the physical and chemical properties, a canonical redundancy analysis (RDA) was performed (Figure 8). A total of 32.1% of the variance in combined benthic fluxes of NH_4^+ and PO_4^{3-} was explained by the eleven selected parameters (permutation test: F = 7.99; $p = 0.001$). The first canonical axis (F = 59.55; $p = 0.001$) represents 64.6% of the constrained variance (20.7% of the total variance) of benthic fluxes data, and is explained by Fe-P ($r = 0.67$; $p = 0.043$), porosity ($r = 0.65$; $p = 0.014$), P-Org ($r = 0.62$; $p = 0.021$), Fecal markers ($r = 0.61$; $p = 0.001$), $\delta^{15}N$ values ($r = 0.42$; $p = 0.02$) and Microalgal markers ($r = 0.38$; $p = 0.001$). The second canonical axis (F = 32.63; $p = 0.001$) represents 35.4% of the constrained variance (11.4% of total) of benthic fluxes data, and is mainly explained by the $\delta^{13}C$ values ($r = -0.76$; $p = 0.002$), followed by Petroleum products markers ($r = -0.40$; $p = 0.001$). The NH_4^+ fluxes were positively correlated with the first axis ($r = 0.64$) and negatively with the second axis ($r = -0.77$). The PO_4^{3-} fluxes were positively correlated with the first axis ($r = 0.77$) and the second axis ($r = 0.64$). Finally, the RDA showed a positive association between the PO_4^{3-} fluxes and the Org-P and Fe-P contents as well as the proportions of fecal markers. For the NH_4^+ fluxes, a positive association was observed with $\delta^{13}C$ and $\delta^{15}N$ values, the porosity and the proportions of microalgal and petroleum product markers.

4. Discussion

4.1. *What is the spatial variability in the origin of SOM?*

In the investigated mudflats, the SOM originated from several natural and anthropogenic sources.

The natural OM sources included terrestrial plants, bacteria, freshwater algae, marine phytoplankton, microphytobenthos, as well as *Ulva* sp., a green macroalgae highly present along the coast of Brittany. From 2008 to 2020, the average surface of stranded *Ulva* on mudflats was 1284 ha (Environmental Observatory of Brittany). The lipids present in the mudflats of Brittany were mainly of natural origin. Their proportion, including ubiquist compounds from natural sources such as cholesterol and LMW FAc, ranged from 24% (Auray River, site #39) to 97% (Ria Etel, site #6) of the analyzed compounds with a mean value of 81 ± 15% (mean ± SD) (%Nat—Figure 9). The isotopic data and the distribution of *n*-alkanes indicated spatial variations of the contribution of these primary producers to the SOM. From middle estuaries to bays, $\delta^{15}N$ values and TAR decreased while $\delta^{13}C$ values and Paq increased with significant differences between bays, lower estuaries and middle estuaries, with the exception of TAR for which the only significant difference was between bays and middle estuaries.

Based on the isotopic shift between C3 terrestrial plants [$\delta^{13}C = -28.7 \pm 0.5$‰ Davoult et al., 2017, Meyers, 1994] and marine organisms [phytoplankton $\delta^{13}C = -21.3 \pm 1.2$‰; Liénart et al., 2017 and *Ulva* sp. $\delta^{13}C = -15.8 \pm 4.4$‰; Berto et al., 2013, Dubois et al., 2012, Riera et al., 1996], the increase in $\delta^{13}C$ values along the estuaries was associated to an increasing proportion of marine OM. This was reinforced by the correlations between $\delta^{13}C$ values and the proportion of terrestrial markers among identified compounds (%Terr—Figure 9) ($r = -0.33$; $p < 0.0001$), the Paq ($r = 0.53$; $p < 0.0001$) and TAR ($r = -0.39$; $p < 0.0001$) ratios quantifying the terrestrial versus aquatic or marine origin of *n*-alkanes. From middle estuaries to bays the proportion of aquatic, calculated using the Paq ratio, and marine, calculated using the TAR ratio, *n*-alkanes increased, indicating an increase in the proportion of SOM inherited from marine organisms, which was recorded by the rise in $\delta^{13}C$ values. Such a trend was in accordance with observations in other estuaries around the world [Ankit et al., 2017, Chevalier et al., 2015, Gireeshkumar et al., 2015, Lopes dos Santos and Vane, 2020].

Microbial transformations of nitrogen induce changes in $\delta^{15}N$ values due to the enzymatic preference for the lighter ^{14}N. Therefore, the anthropogenic inputs from WWTP and agriculture, subject
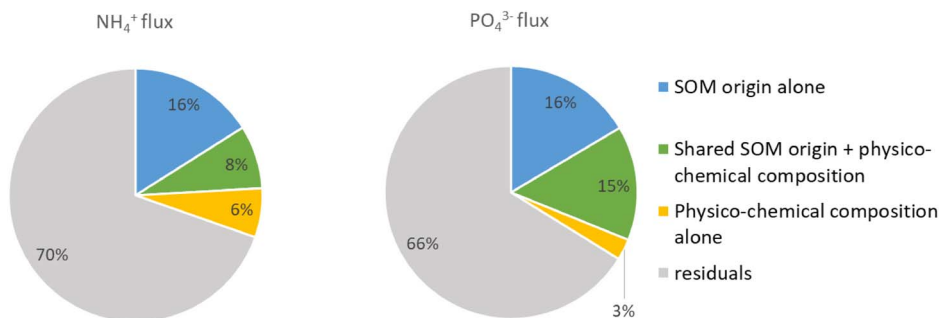
Figure 7. Variation partitioning of the NH_4^+ and PO_4^{3-} fluxes. "SOM origin" corresponds to $\delta^{13}C$ values, $\delta^{15}N$ values and the proportions of the lipid marker groups. "Physico-chemical composition" corresponds to the selected parameters related to the composition (Fe-P, Org-P) and physical properties (porosity) of the sediment.
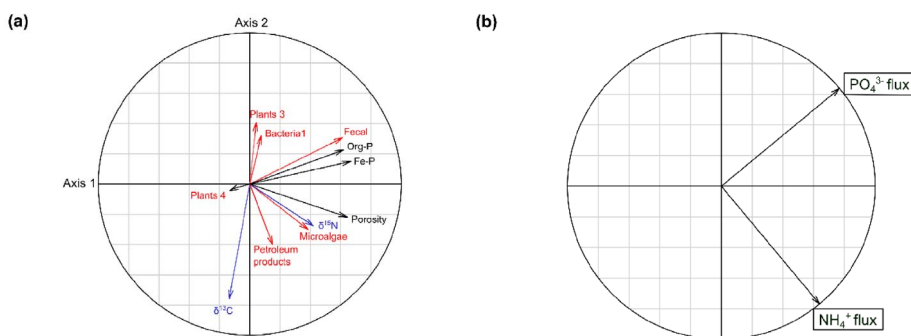

Figure 8. Correlation circles of the Canonical Redundancy Analysis (RDA) showing the correlations between (a) the explanatory variables, related to the SOM origin (in red), isotopic composition (in blue) and physico-chemical properties (in black) of the sediment, and (b) the response variables (NH_4^+ and PO_4^{3-} fluxes).

to microbial activity, generally show an increase in adjacent sedimentary $\delta^{15}N$ values [Finlay and Kendall, 2007, Rumolo et al., 2011, Savage, 2005]. The occurrence of WWTP, individual septic systems and the elevated agricultural density (80% of the area) are both potential sources in the current study. When considering all the samples, $\delta^{15}N$ values negatively correlated with the Paq n-alkane ratio ($r = -0.34$, $p < 0.0001$). High $\delta^{15}N$ values were associated with high proportion of terrigenous n-alkanes. Since Brittany is a highly agricultural area, we assume that terrigenous n-alkanes were indicators of soil erosion and thus of agricultural inputs. $\delta^{15}N$ values were also positively correlated with the proportion of human fecal stanols among analyzed compounds ($r = 0.15$, $p = 0.035$). Consequently the $\delta^{15}N$ values indicated that mudflats of Brittany would be

influenced by both waste water management and agricultural practices.

Overall, the correlations between isotopic and lipid data were relatively weak, which could be due to the fact that isotopic data result from the combination of all the sources of OM (natural and anthropogenic ones). Lipid analysis highlighted four sources of anthropogenic OM. Two are characteristic of petroleum products: diesel and potentially degraded crude oil. Both of these contaminations occurred in all mudflat sediments with variable proportions as indicated by the ratio diesel/petrogenic (%Diesel—Figure 9). The petrogenic contamination was mainly due to crude oil in Northern mudflats, while diesel dominated in Southern mudflats, with the exception of the Rance Estuary in the north, the Lorient Bay and the Ria d'Etel in the south. Compared
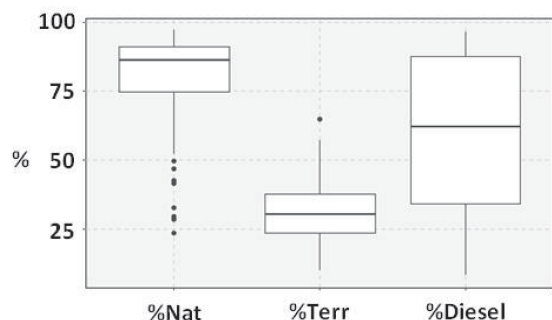
Figure 9. Ranges of variation of ratios calculated on the distribution of lipids. %Nat is the proportion of natural markers among all identified compounds, including ubiquist compounds. %Terr is the proportion of terrigenous markers among all identified compounds, including ubiquist compounds. %Diesel is the proportion of diesel markers among petrogenic markers.

to Northern mudflats, the Rance Estuary sediments were enriched with diesel ($p < 0.01$), which could be due to the low hydrodynamics induced by the tidal power plant that closes this estuary since the 60's [Rtimi et al., 2021]. Compared to Southern mudflats, the concentration of diesel markers were lower in the Lorient Bay ($p < 0.001$) and the Ria d'Etel ($p < 0.001$). Since the land use is very similar in upstream areas along the southern coast, these differences could be due to a combination of geomorphological and hydrological conditions that could impact the sedimentation of diesel droplets [Gearing et al., 1980].

The third source of anthropogenic OM was pyrogenic and was characterized by the occurrence and the distribution of PAHs [Yunker et al., 2002]. Its occurrence in mudflat sediments, quantified by the sum of the concentration of the 16 PAHs listed by the US-Environmental Protection Agency (US-EPA) was in the same range but slightly higher than in the European Northern Sea and the Baltic Sea [Wang et al., 2020]. The background contamination in sediments of the eastern North Atlantic has been determined by the OSPAR commission, a cooperation between 15 governments and the European Union to protect the marine environment of the North-East Atlantic (OSPAR, 2017). Among the present samples, 24% of the mudflat sediments presented higher contamination levels than this background. Most of these were

from the Ria d'Etel (25% of the contaminated sediments), Auray River (23%) and Lorient Bay (21%). Isomeric ratios calculated on PAH allowed identifying particles coming from the emissions from road traffic and aged by photolysis as the main pyrogenic source (Figure S3). This was in agreement with one of the main source of PAHs identified in Northern and Baltic seas [Wang et al., 2020].

Finally, the anthropogenic OM from fecal contaminations was highlighted by the occurrence and the distribution of fecal stanols. The sum of their concentrations ranged from 4 to 1934 ng/g of dry sediment (276 ± 261 ng/g; mean $\pm$ sd). This was 10 times lower than in the Tay Estuary (Scotland) before the building of a WWTP [Reeves and Patton, 2005] and 5 times lower than the mean concentrations in Jinhae Bay (South Korea) [Choi et al., 2002]. Only 4 samples of the study exhibited a coprostanol concentration higher than 500 ng/g, which has been suggested as the threshold to indicate a significant fecal contamination [Leeming and Nichols, 1996]. Based on this, fecal contamination was small in mudflat sediments along the Brittany coastline. This fecal contamination resulted mainly from cow manure ($68 \pm 14\%$) and pig slurry ($11 \pm 15\%$) exports and inputs from WWTP effluent or non-connected installations ($21 \pm 8\%$), which was in accordance to the combination of sources of fecal contamination that has been determined in rivers of Brittany [Jardé et al., 2018].

4.2. *How the origin of SOM impacts benthic nutrient fluxes?*

The origin of SOM has often been suggested as a driver of SOM biodegradation and benthic nutrient fluxes [LaRowe et al., 2020]. This large dataset allowed for the first time to significantly quantify this relationship for NH_4^+ and PO_4^{3-} fluxes produced by mudflats in tidal environments. The benthic NH_4^+ and PO_4^{3-} fluxes, measured from the sediment core incubations, were significantly correlated ($p < 0.005$) to the SOM origin. The percentage of variance for the NH_4^+ and PO_4^{3-} fluxes explained only by the "SOM origin" variables was 16%, compared to 6% (for NH_4^+ fluxes) and 3% (for PO_4^{3-} fluxes) for the "physico-chemical composition" variables. By combining all variables, the explained percentage of variance for the NH_4^+ and PO_4^{3-} fluxes reached 30 and

34% respectively. The origin of SOM was thus a significant driver of benthic nutrient fluxes. The RDA highlighted that the NH_4^+ and PO_4^{3-} fluxes were not correlated to the same variables.

The NH_4^+ flux was positively related to the isotopic signature of the bulk sediment OM ($\delta^{15}N$ and $\delta^{13}C$ values), the porosity and the proportions of microalgal and diesel markers. In geographically closed areas, low hydrodynamic conditions improve the sedimentation of (i) fine particles, increasing the porosity of sediments [Meade, 1966] and (ii) diesel droplets lighter than seawater through flocculation. In such low hydrodynamic conditions, the development of microalgae promoted by anthropogenic N coming from watersheds and their sedimentation must have brought to the sediment ^{13}C-enriched [Cook et al., 2004, Li et al., 2016, Ogrinc et al., 2005] and ^{15}N-enriched [Savage, 2005, Finlay and Kendall, 2007, Rumolo et al., 2011] marine OM, increasing the proportion of microalgal markers in the lipidic fraction of SOM. Phytoplanktonic blooms are known to enrich sediments in nitrogen and labile SOM [Franzo et al., 2019]. These inputs have promoted a quick response of the bacterial reactivity in the sediment [Hardison et al., 2013, Pruski et al., 2019], which has induced seasonal variability in benthic nitrogen fluxes [Grenz et al., 2000]. The present results showed that phytoplanktonic blooms could also be responsible for spatial variability in benthic nitrogen fluxes from mudflat sediments. The NH_4^+ flux was thus partially controlled by the origin of SOM that might have been driven by the geomorphology. Under low hydrodynamic conditions, an algal bloom might have been stimulated, especially if the coastal system was impacted by nitrogen loading from the watershed, and thus become an OM source for the coastal sediment.

The geographical configuration of the Gulf of Morbihan which opens onto the Atlantic Ocean through a narrow passage 850 m wide and covering an area of 115 km^2 illustrated perfectly these relationships between geomorphology, origin of SOM and benthic NH_4^+ flux. This area combined the samples from the Auray River, Vannes and the southern internal coast of the Gulf (Figure 1). In this area, the porosity was significantly higher ($p < 0.0001$) than in other mudflats, which indicated an area with low hydrodynamic conditions. These conditions have improved the assimilation of dissolved anthropogenic nitrogen by microalgae and their sedimentation. Higher sed-

imentation rates were emphasized by significantly higher proportions of diesel markers in this area ($p < 0.0001$). As a consequence, SOM was enriched in OM from microalgae as indicated by significantly higher $\delta^{15}N$ ($p < 0.01$), $\delta^{13}C$ ($p < 0.0001$) and microalgal markers ($p < 0.001$), which induced a mean NH_4^+ flux that was two times higher than in the other mudflats of Brittany ($p = 0.001$).

This link between topography, algal bloom, sedimentation and enrichment in sedimentary heavy nitrogen seems in accordance with the main mode of export of nitrogen from agricultural watersheds that is mainly under dissolved form [Mulholland et al., 2008]. Before storage in mudflat sediments, N must be fixed by aquatic primary producers. In 2021, the mean Q90 (the value below which at least 90% of the data fall) nitrate concentration at the regional scale was 41 ± 25 mg/L (data from the Environment Observatory in Brittany). Consequently, reducing benthic N fluxes from mudflat sediments will require a decrease in the dissolved N fluxes from agricultural catchments and then a decrease in the amount of N fertilizers used by the chemical conventional agriculture to avoid N-surplus [Leip et al., 2011].

The PO_4^{3-} flux was positively related to the proportion of fecal markers, as well as the Org-P and Fe-P. Fecal markers occurring in the investigated mudflats originated mainly from the erosion of agricultural soils amended with bovine manure and pig slurry ($79 \pm 29\%$) and from WWTP and individual septic systems ($21 \pm 8\%$). This finding seems to be in accordance with the increase in PO_4^{3-} fluxes via a larger dissolution rate of Fe-P due to reductive conditions in sediments impacted by urban and agricultural activities in the Bay of Brest in Brittany [Khalil et al., 2018]. Biogeochemical modelling used to investigate the mechanisms behind these relationships has highlighted the role of the input of labile OM from urban and agricultural activities. This would have led to high mineralization rates and in the increase in PO_4^{3-} fluxes through both mineralization and subsequent reductive Fe-P dissolution [Ait Ballagh et al., 2020].

Org-P and Fe-P in sediments may come from direct sedimentation of particulate Org-P and Fe-P exported by watersheds or from sedimentation of marine primary producers that would have assimilated dissolved P [Watson et al., 2018]. In rivers of Brittany, over the period 2007 to 2011, the mean fluxes of particulate P has been 1.7 times higher than the mean

fluxes of dissolved P [Bol et al., 2018]. The correlations between sedimentary P stocks and $\delta^{13}C$ (Org-P: $r = -0.21$, $p < 0.01$; Fe-P: $r = -0.32$, $p < 0.001$), Paq (Org-P: $r = -0.27$, $p < 0.001$; Fe-P: $r = -0.30$, $p < 0.001$) and the concentration of fecal markers (Org-P: $r = 0.40$, $p < 0.001$; Fe-P: $r = 0.37$, $p < 0.001$) seems to indicate that sedimentary P stocks were mainly associated with terrestrial OM. This could highlight particulate P as the main source of sedimentary P through soil erosion. Moreover the median benthic PO_4^{3-} fluxes were positively correlated to the watershed area ($r = 0.8$, $p < 0.001$). Intensive agricultural activities cover 60% of the area in Brittany and result in one of the world's largest P surpluses [MacDonald et al., 2011], which may affect the sediment composition through agricultural soil erosion, which can be considered as a transport vector of fecal matter and particulate phosphorus. Therefore, benthic PO_4^{3-} fluxes seem to be driven by the surface area of the watersheds and the land use in the catchment. Consequently, agricultural practices allowing a decrease in P surplus and soil erosion should induce a decrease in sedimentary P stocks and then a decrease in benthic PO_4^{3-} fluxes.

4.3. *A large proportion of the variance of benthic nutrient fluxes remained unexplained*

In the present study, we focused on the link between the benthic nutrient fluxes and the sediment composition, while comparing the significant effect of SOM origin versus quantity. Nevertheless, a large part of the variance in the benthic NH_4^+ and PO_4^{3-} fluxes on the regional scale remained unexplained (70 and 66%, respectively) (Figure 7). Microbial abundance and diversity were not assessed in the current study, and abundance and/or diversity may play an additional role in nutrient cycling. As shown by Abell et al. [2013], the composition of the bacterial community has been related to the nature of the OM in estuarine systems, and their combination may lead to a shift in the benthic nutrient fluxes. In addition, bioturbation, mediated by macrofauna activities, was likely present in the sediment core incubations and possibly involved in the spatial variability of the NH_4^+ and PO_4^{3-} fluxes. Bioturbation includes particle reworking and burrow ventilation, promoting exchanges of solute between the porewater and the overlying water and stimulating microbial activities [Graf and Rosenberg,

1997]. The review and experimental studies of Karlson et al. [2007] and Renz and Forster [2014] have highlighted the stimulation of the NH_4^+ and PO_4^{3-} effluxes by benthic macrofauna, with a magnitude that varied according to the density, burrowing depth and ventilation of polychaetes and bivalves. Bioturbation promotes NH_4^+ effluxes through the mineralization of SOM via an additional supply of electron acceptors (e.g. oxygen, nitrate), the remobilization of burial OM, and NH_4^+ excretion from macrofauna [Welsh, 2003, and references therein]). The release of PO_4^{3-} in the presence of macrofauna also depends on the sediment redox status and components (e.g iron oxides). In fact, bioturbation increases P-Org mineralization and then regenerated PO_4^{3-} can be either released by porewater flushing or adsorbed into iron oxides under oxic conditions. Therefore, Nizzoli et al. [2007] observed that the bioturbation by polychaete *Nereis* spp. had site specific effects on the flux, with sediment acting either as a sink or a source of PO_4^{3-}.

5. Conclusion

To the best of our knowledge, this is the first study that describes the variability in the SOM origin through a broad sampling campaign of marine mudflats at the regional scale (Brittany), relating SOM origin to benthic nutrient fluxes. The combination of isotopic and lipid data emphasized the SOM in Brittany intertidal mudflats as a mixture of natural (marine and continental) and anthropogenic OM. Its composition varied according to the anthropogenic pressures of watersheds as well as the hydrodynamic conditions. Benthic nutrient fluxes were significantly driven by the origin of SOM that explained 24% and 31% of the variance of NH_4^+ and PO_4^{3-} fluxes, respectively. Benthic nutrient fluxes were linked to terrestrial export of N and P but were not correlated to the same parameters. The NH_4^+ fluxes were driven by the uptake by phytoplankton of dissolved anthropogenic N exported from agricultural catchments. Their sedimentation was favoured by low hydrodynamic conditions, enriching the sediments with labile OM. The PO_4^{3-} fluxes were driven by the sedimentation of particulate P exported through agricultural soil erosion.

A significant fraction of the spatial variability in the benthic nutrient fluxes remains unexplained by the investigated sedimentary characteristics. The spatial variability of benthic macrofauna and

microbial biomass might play a role in this unexplained variance and should be considered in future investigations.

Conflicts of interest

The authors declare that they have no conflict of interest.

Acknowledgments

Supplementary data

Supporting information for this article is available on the journal's website under https://doi.org/10.5802/crgeos.228 or from the author.

References

Abell, G. C. J., Ross, D. J., Keane, J. P., Oakes, J. M., Eyre, B. D., Robert, S. S., and Volkman, J. K. (2013). Nitrifying and denitrifying microbial communities and their relationship to nutrient fluxes and sediment geochemistry in the Derwent Estuary, Tasmania. *Aquat. Microb. Ecol.*, 70, 63–75.

Ait Ballagh, F. E., Rabouille, C., Andrieux-Loyer, F., Soetaert, K., Elkalay, K., and Khalil, K. (2020). Spatio-temporal dynamics of sedimentary phosphorus along two temperate eutrophic estuaries: A data-modelling approach. *Cont. Shelf Res.*, 193, article no. 104037.

Akbarzadeh, Z., Laverman, A. M., Rezanezhad, F., Raimonet, M., Viollier, E., Shafei, B., and Van Cappellen, P. (2018). Benthic nitrite exchanges in the Seine River (France): An early diagenetic modeling analysis. *Sci. Total Environ.*, 628–629, 580–593.

Albert, S., Bonaglia, S., Stjärnkvist, N., Winder, M., Thamdrup, B., and Nascimento, F. J. A. (2021). Influence of settling organic matter quantity and quality on benthic nitrogen cycling. *Limnol. Oceanogr.*, 66, 1882–1895.

Anderson, I. C., McGlathery, K. J., and Tyler, A. C. (2003). Microbial mediation of "reactive" nitrogen transformations in a temperate lagoon. *Mar. Ecol. Prog. Ser.*, 246, 73–84.

Andrieux-Loyer, F., Azandegbé, A., Caradec, F., Philippon, X., Kérouel, R., Youenou, A., and Nicolas, J.-L. (2014). Impact of oyster farming on diagenetic processes and the phosphorus cycle in two estuaries (Brittany, France). *Aquat. Geochem.*, 20, 573–611.

Ankit, Y., Mishra, P. K., Kumar, P., Jha, D. K., Kumar, V. V., Ambili, V., and Anoop, A. (2017). Molecular distribution and carbon isotope of *n*-alkanes from Ashtamudi Estuary, South India: Assessment of organic matter sources and paleoclimatic implications. *Mar. Chem.*, 196, 62–70.

Arndt, S., Jørgensen, B. B., LaRowe, D. E., Middelburg, J. J., Pancost, R. D., and Regnier, P. (2013). Quantifying the degradation of organic matter in marine sediments: A review and synthesis. *Earth-Sci. Rev.*, 123, 53–86.

Berto, D., Rampazzo, F., Noventa, S., Cacciatore, F., Gabellini, M., Aubry, F. B., Girolimetto, A., and Brusà, R. B. (2013). Stable carbon and nitrogen isotope ratios as tools to evaluate the nature of particulate organic matter in the Venice lagoon. *Estuar. Coast. Shelf Sci.*, 135, 66–76.

Bianchi, T. S. and Bauer, J. E. (2011). 5.03 - particulate organic carbon cycling and transformation. In Wolanski, E. and McLusky, D., editors, *Treatise on Estuarine and Coastal Science*, pages 69–117. Academic Press, Waltham.

Bol, R., Gruau, G., Mellander, P.-E., Dupas, R., Bechmann, M., Skarbøvik, E., Bieroza, M., Djodjic, F.,

Glendell, M., Jordan, P., Van der Grift, B., Rode, M., Smolders, E., Verbeeck, M., Gu, S., Klumpp, E., Pohle, I., Fresne, M., and Gascuel-Odoux, C. (2018). Challenges of reducing phosphorus based water eutrophication in the agricultural landscapes of Northwest Europe. *Front. Mar. Sci.*, 5, article no. 276.

Borcard, D., Gillet, F., and Legendre, P. (2018). *Numerical Ecology with R*. Springer, New York, NY.

Borcard, D., Legendre, P., and Drapeau, P. (1992). Partialling out the spatial component of ecological variation. *Ecology*, 73, 1045–1055.

Bourbonniere, R. A. and Meyers, P. A. (1996). Sedimentary geolipid records of historical changes in the watersheds and productivities of Lakes Ontario and Erie. *Limnol. Oceanogr.*, 41, 352–359.

Boynton, W. R., Ceballos, M. A. C., Bailey, E. M., Hodgkins, C. L. S., Humphrey, J. L., and Testa, J. M. (2018). Oxygen and nutrient exchanges at the sediment-water interface: a global synthesis and critique of estuarine and coastal data. *Estuar. Coast.*, 41, 301–333.

Brassel, S. C., Eglinton, G., Maxwell, J. R., and Philip, R. P. (1978). Natural background of alkanes in the aquatic environment. In Hutzinger, O., Van Leleyveld, I. H., and Zoeteman, B. C. J., editors, *Aquatic Pollutants*, pages 69–86. Pergamon Press, Oxford.

Bray, E. E. and Evans, E. D. (1961). Distribution of *n*-paraffins as a clue to recognition of source beds. *Geochim. Cosmochim. Acta*, 22, 2–15.

Chevalier, N., Savoye, N., Dubois, S., Lama, M. L., David, V., Lecroart, P., le Ménach, K., and Budzinski, H. (2015). Precise indices based on *n*-alkane distribution for quantifying sources of sedimentary organic matter in coastal systems. *Org. Geochem.*, 88, 69–77.

Choi, H. G., Kim, S. G., Kim, S. S., Moon, H. B., Lee, P. Y., and Park, C. K. (2002). Sterols of sewage indicators in marine sediments of Jinhae Bay, Korea. *J. Kor. Soc. Oceanogr.*, 37, 551–557.

Cook, P. L. M., Revill, A. T., Clementson, L. A., and Volkman, J. K. (2004). Carbon and nitrogen cycling on intertidal mudflats of a temperate Australian estuary. III. Sources of organic matter. *Mar. Ecol. Prog. Ser.*, 280, 55–72.

Cranwell, P. A. (1974). Monocarboxylic acids in lake sediments: Indicators, derived from terrestrial and aquatic biota, of paleoenvironmental trophic levels. *Chem. Geol.*, 14, 1–14.

Cranwell, P. A., Eglinton, G., and Robinson, N. (1987). Lipids of aquatic organisms as potential contributors to lacustrine sediments—II. *Org. Geochem.*, 11, 513–527.

Davoult, D., Surget, G., Stiger-Pouvreau, V., Noisette, F., Riera, P., Stagnol, D., Androuin, T., and Poupart, N. (2017). Multiple effects of a Gracilaria vermiculophylla invasion on estuarine mudflat functioning and diversity. *Mar. Environ. Res.*, 131, 227–235.

Derrien, M., Jardé, E., Gruau, G., and Pierson-Wickmann, A.-C. (2011). Extreme variability of steroid profiles in cow feces and pig slurries at the regional scale: implications for the use of steroids to specify fecal pollution sources in waters. *J. Agric. Food Chem.*, 59, 7294–7302.

Derrien, M., Jardé, E., Gruau, G., Pourcher, A. M., Gourmelon, M., Jadas-Hécart, A., and Pierson Wickmann, A. C. (2012). Origin of fecal contamination in waters from contrasted areas: Stanols as Microbial Source Tracking markers. *Water Res.*, 46, 4009–4016.

Derrien, M., Yang, L., and Hur, J. (2017). Lipid biomarkers and spectroscopic indices for identifying organic matter sources in aquatic environments: A review. *Water Res.*, 112, 58–71.

Dubois, S., Savoye, N., Grémare, A., Plus, M., Charlier, K., Beltoise, A., and Blanchet, H. (2012). Origin and composition of sediment organic matter in a coastal semi-enclosed ecosystem: An elemental and isotopic study at the ecosystem space scale. *J. Mar. Syst.*, 94, 64–73.

Eglinton, G. and Hamilton, R. J. (1967). Leaf epicuticular waxes. *Science*, 156, 1322–1335.

Ficken, K. J., Li, B., Swain, D. L., and Eglinton, G. (2000). An *n*-alkane proxy for the sedimentary input of submerged/floating freshwater aquatic macrophytes. *Org. Geochem.*, 31, 745–749.

Finlay, J. C. and Kendall, C. (2007). Stable isotope tracing of temporal and spatial variability in organic matter sources to freshwater ecosystems. In Michener, R. and Lajtha, K., editors, *Stable Isotopes in Ecology and Environmental Science*, pages 283–333. Blackwell Publishing Ltd, Oxford, UK.

Flint, R. W. and Kamykowski, D. (1984). Benthic nutrient regeneration in South Texas coastal waters. *Estuar. Coast. Shelf Sci.*, 18, 221–230.

Franzo, A., Celussi, M., Bazzaro, M., Relitti, F., and Del Negro, P. (2019). Microbial processing of sedimentary organic matter at a shallow LTER site in the northern Adriatic Sea: an 8-year case study. *Nat. Conserv.*, 34, 397–415.

Freese, E., Köster, J., and Rullkötter, J. (2008). Origin and composition of organic matter in tidal flat sediments from the German Wadden Sea. *Org. Geochem.*, 39, 820–829.

Freitas, F. S., Pika, P. A., Kasten, S., Jørgensen, B. B., Rassmann, J., Rabouille, C., Thomas, S., Sass, H., Pancost, R. D., and Arndt, S. (2021). New insights into large-scale trends of apparent organic matter reactivity in marine sediments and patterns of benthic carbon transformation. *Biogeosci.*, 18, 4651–4679.

Gearing, P. J., Gearing, J. N., Pruell, R. J., Wade, T. L., and Quinn, J. G. (1980). Partitioning of no. 2 fuel oil in controlled estuarine ecosystems. Sediments and suspended particulate matter. *Environ. Sci. Technol.*, 14, 1129–1136.

Gireeshkumar, T. R., Deepulal, P. M., and Chandramohanakumar, N. (2015). Distribution and sources of aliphatic hydrocarbons and fatty acids in surface sediments of a tropical estuary south west coast of India (Cochin estuary). *Environ. Monit. Assess.*, 187, article no. 56.

Graf, G. and Rosenberg, R. (1997). Bioresuspension and biodeposition: a review. *J. Mar. Syst.*, 11, 269–278.

Grenz, C., Cloern, J. E., Hager, S. W., and Cole, B. E. (2000). Dynamics of nutrient cycling and related benthic nutrient and oxygen fluxes during a spring phytoplankton bloom in South San Francisco Bay (USA). *Mar. Ecol. Prog. Ser.*, 197, 67–80.

Hardison, A. K., Canuel, E. A., Anderson, I. C., Tobias, C. R., Veuger, B., and Waters, M. N. (2013). Microphytobenthos and benthic macroalgae determine sediment organic matter composition in shallow photic sediments. *Biogeosci.*, 10, 5571–5588.

Iatrides, M. C., Artaud, J., and Vicente, N. (1983). Composition en stérols de végétaux marins méditerranéens. *Oceanol. Acta*, 6, 73–77.

Jaffé, R., Mead, R., Hernandez, M. E., Peralba, M. C., and DiGuida, O. A. (2001). Origin and transport of sedimentary organic matter in two subtropical estuaries: a comparative, biomarker-based study. *Org. Geochem.*, 32, 507–526.

Jardé, E., Jeanneau, L., Harrault, L., Quenot, E.,

Solecki, O., Petitjean, P., Lozach, S., Chevé, J., and Gourmelon, M. (2018). Application of a microbial source tracking based on bacterial and chemical markers in headwater and coastal catchments. *Sci. Total Environ.*, 610–611, 55–63.

Jeanneau, L., Faure, P., and Montarges-Pelletier, E. (2008). Quantitative multimolecular marker approach to investigate the spatial variability of the transfer of pollution from the Fensch River to the Moselle River (France). *Sci. Total Environ.*, 389, 503–513.

Karlson, K., Bonsdorff, E., and Rosenberg, R. (2007). The impact of benthic macrofauna for nutrient fluxes from baltic sea sediments. *Ambio*, 36, 161–167.

Katsoyiannis, A., Terzi, E., and Cai, Q.-Y. (2007). On the use of PAH molecular diagnostic ratios in sewage sludge for the understanding of the PAH sources. Is this use appropriate? *Chemosphere*, 69, 1337–1339.

Khalil, K., Laverman, A. M., Raimonet, M., and Rabouille, C. (2018). Importance of nitrate reduction in benthic carbon mineralization in two eutrophic estuaries: Modeling, observations and laboratory experiments. *Mar. Chem.*, 199, 24–36.

LaRowe, D. E., Arndt, S., Bradley, J. A., Estes, E. R., Hoarfrost, A., Lang, S. Q., Lloyd, K. G., Mahmoudi, N., Orsi, W. D., Shah Walter, S. R., Steen, A. D., and Zhao, R. (2020). The fate of organic carbon in marine sediments - New insights from recent data and analysis. *Earth-Sci. Rev.*, 204, article no. 103146.

Lee, C.-B. and Kim, D.-S. (1990). Pore water chemistry of intertidal mudflat sediments: 1. Seasonal variability of nutrient profiles (S, N, P). *J. Oceanol. Soc. Korea*, 25, 8–20.

Leeming, R., Ball, A., Ashbolt, N., and Nichols, P. D. (1996). Using faecal sterols from humans and animals to distinguish faecal pollution in receiving waters. *Water Res.*, 30, 2893–2900.

Leeming, R. and Nichols, P. D. (1996). Concentrations of coprostanol that correspond to existing bacterial indicator guideline limits. *Water Res.*, 30, 2997–3006.

Leip, A., Achermann, B., Billen, G., Bleeker, A., Bouwman, A., de Vries, W., Dragosits, U., Doring, U., Fernall, D., Geupel, M., Herolstab, J., Johnes, P., Le Gall, A. C., Monni, S., Neveceral, R., Orlandini, L., Prud'homme, M., Reuter, H., Simpson, D., Seufert, G., Spranger, T., Sutton, M., van Aardenne, J., Voss,

M., and Winiwarter, W. (2011). Integrating nitrogen fluxes at the European scale. In Sutton, M., Howard, C., Erisman, J. W., Billen, G., Bleeker, A., Greenfelt, P., van Grinsven, H., and Grizzette, B., editors, *The European Nitrogen Assessment*, pages 345–376. Cambridge University Press, Cambridge. ISBN 9781107006126. Available at https://centaur.reading.ac.uk/28386/.

Li, Y., Zhang, H., Tu, C., Fu, C., Xue, Y., and Luo, Y. (2016). Sources and fate of organic carbon and nitrogen from land to ocean: Identified by coupling stable isotopes with C/N ratio. *Estuar. Coast. Shelf Sci.*, 181, 114–122.

Liénart, C., Savoye, N., Bozec, Y., Breton, E., Conan, P., David, V., Feunteun, E., Grangeré, K., Kerhervé, P., Lebreton, B., Lefebvre, S., L'Helguen, S., Mousseau, L., Raimbault, P., Richard, P., Riera, P., Sauriau, P.-G., Schaal, G., Aubert, F., Aubin, S., Bichon, S., Boinet, C., Bourasseau, L., Bréret, M., Caparros, J., Cariou, T., Charlier, K., Claquin, P., Cornille, V., Corre, A.-M., Costes, L., Crispi, O., Crouvoisier, M., Czamanski, M., Del Amo, Y., Derriennic, H., Dindinaud, F., Durozier, M., Hanquiez, V., Nowaczyk, A., Devesa, J., Ferreira, S., Fornier, M., Garcia, F., Garcia, N., Geslin, S., Grossteffan, E., Gueux, A., Guillaudeau, J., Guillou, G., Joly, O., Lachaussée, N., Lafont, M., Lamoureux, J., Lecuyer, E., Lehodey, J.-P., Lemeille, D., Leroux, C., Macé, E., Maria, E., Pineau, P., Petit, F., Pujo-Pay, M., Rimelin-Maury, P., and Sultan, E. (2017). Dynamics of particulate organic matter composition in coastal systems: A spatio-temporal study at multi-systems scale. *Prog. Oceanogr.*, 156, 221–239.

Lopes dos Santos, R. A. and Vane, C. H. (2020). Molecular and bulk geochemical proxies in sediments from the Conwy Estuary, UK. *Org. Geochem.*, 150, article no. 104119.

López-Rosales, A. R., Ancona-Canché, K., Chavarria-Hernandez, J. C., Barahona-Pérez, F., Toledano-Thompson, T., Garduño Solórzano, G., López-Adrian, S., Canto-Canché, B., Polanco-Lugo, E., and Valdez-Ojeda, R. (2019). Fatty acids, hydrocarbons and terpenes of *Nannochloropsis* and *Nannochloris* isolates with potential for biofuel production. *Energies*, 12, article no. 130.

Louis, J., Jeanneau, L., Andrieux-Loyer, F., Gruau, G., Caradec, F., Lebris, N., Chorin, M., Jardé, E., Rabiller, E., Petton, C., Bouger, G., Petitjean, P., and Laverman, A. M. (2021). Are benthic nutrient fluxes from intertidal mudflats driven by surface sediment characteristics? *C. R. Geosci.*, 353, 173–191.

MacDonald, G. K., Bennett, E. M., Potter, P. A., and Ramankutty, N. (2011). Agronomic phosphorus imbalances across the world's croplands. *Proc. Natl. Acad. Sci. USA*, 108, 3086–3091.

Meade, R. H. (1966). Factors influencing early stages of compaction of clays and sands—review. *AAPG Bull.*, 50, 626–627.

Ménesguen, A., Dussauze, M., Dumas, F., Thouvenin, B., Garnier, V., Lecornu, F., and Répécaud, M. (2019). Ecological model of the Bay of Biscay and English Channel shelf for environmental status assessment part 1: Nutrients, phytoplankton and oxygen. *Ocean Model.*, 133, 56–78.

Mesnage, V., Ogier, S., Bally, G., Disnar, J.-R., Lottier, N., Dedieu, K., Rabouille, C., and Copard, Y. (2007). Nutrient dynamics at the sediment-water interface in a Mediterranean lagoon (Thau, France): Influence of biodeposition by shellfish farming activities. *Mar. Environ. Res.*, 63, 257–277.

Meyers, P. A. (1994). Preservation of elemental and isotopic source identification of sedimentary organic matter. *Chem. Geol.*, 114, 289–302.

Meziane, T. and Tsuchiya, M. (2000). Fatty acids as tracers of organic matter in the sediment and food web of a mangrove/intertidal flat ecosystem, Okinawa, Japan. *Mar. Ecol. Prog. Ser.*, 200, 49–57.

Mulholland, P. J., Helton, A. M., Poole, G. C., Hall, R. O., Hamilton, S. K., Peterson, B. J., Tank, J. L., Ashkenas, L. R., Cooper, L. W., Dahm, C. N., Dodds, W. K., Findlay, S. E. G., Gregory, S. V., Grimm, N. B., Johnson, S. L., McDowell, W. H., Meyer, J. L., Valett, H. M., Webster, J. R., Arango, C. P., Beaulieu, J. J., Bernot, M. J., Burgin, A. J., Crenshaw, C. L., Johnson, L. T., Niederlehner, B. R., O'Brien, J. M., Potter, J. D., Sheibley, R. W., Sobota, D. J., and Thomas, S. M. (2008). Stream denitrification across biomes and its response to anthropogenic nitrate loading. *Nature*, 452, 202–205.

Nizzoli, D., Bartoli, M., Cooper, M., Welsh, D. T., Underwood, G. J. C., and Viaroli, P. (2007). Implications for oxygen, nutrient fluxes and denitrification rates during the early stage of sediment colonisation by the polychaete Nereis spp. in four estuaries. *Estuar. Coast. Shelf Sci.*, 75, 125–134.

Ogrinc, N., Fontolan, G., Faganeli, J., and Covelli,

S. (2005). Carbon and nitrogen isotope compositions of organic matter in coastal marine sediments (the Gulf of Trieste, N Adriatic Sea): indicators of sources and preservation. *Mar. Chem.*, 95, 163–181.

Oksanen, J., Blanchet, F. G., Kindt, R., Legendre, P., Minchin, P. R., O'hara, R. B., Simpson, G. L., Solymos, P., Stevens, M. H. H., and Wagner, H. (2013). Vegan: community ecology package version 2.0-10. *J. Stat. Softw.*, 48(9), 103–132.

Oliveira, C., Martins, N., Tavares, J., Pio, C., Cerqueira, M., Matos, M., Silva, H., Oliveira, C., and Camões, F. (2011). Size distribution of polycyclic aromatic hydrocarbons in a roadway tunnel in Lisbon, Portugal. *Chemosphere*, 83, 1588–1596.

Ortiz, J. E., Moreno, L., Torres, T., Vegas, J., Ruiz-Zapata, B., García-Cortés, Á., Galán, L., and Pérez-González, A. (2013). A 220 ka palaeoenvironmental reconstruction of the Fuentillejo maar lake record (Central Spain) using biomarker analysis. *Org. Geochem.*, 55, 85–97.

Perrot, T., Rossi, N., Ménesguen, A., and Dumas, F. (2014). Modelling green macroalgal blooms on the coasts of Brittany, France to enhance water quality management. *J. Mar. Syst.*, 132, 38–53.

Peters, K. E. and Moldovan, J. M. (1993). *The Biomarker Guide: Interpreting Molecular Fossils in Petroleum and Ancient Sediment*. Prentice-Hall, Englewood Cliffs.

Pruski, A. M., Buscail, R., Bourrin, F., and Vétion, G. (2019). Influence of coastal Mediterranean rivers on the organic matter composition and reactivity of continental shelf sediments: The case of the Têt River (Gulf of Lions, France). *Cont. Shelf Res.*, 181, 156–173.

Reeves, A. D. and Patton, D. (2005). faecal sterols as indicators of sewage contamination in estuarine sediments of the Tay Estuary, Scotland: an extended baseline survey. *Hydrol. Earth Syst. Sci.*, 9, 81–94.

Renz, J. R. and Forster, S. (2014). Effects of bioirrigation by the three sibling species of Marenzelleria spp. on solute fluxes and porewater nutrient profiles. *Mar. Ecol. Prog. Ser.*, 505, 145–159.

Riera, P., Richard, P., Grémare, A., and Blanchard, G. (1996). Food source of intertidal nematodes in the Bay of Marennes-Oléron (France), as determined by dual stable isotope analysis. *Mar. Ecol. Prog. Ser.*, 142, 303–309.

Rtimi, R., Sottolichio, A., and Tassi, P. (2021). Hydrodynamics of a hyper-tidal estuary influenced by the world's second largest tidal power station (Rance estuary, France). *Estuar. Coast. Shelf Sci.*, 250, article no. 107143.

Rumolo, P., Barra, M., Gherardi, S., Marsella, E., and Sprovieri, M. (2011). Stable isotopes and C/N ratios in marine sediments as a tool for discriminating anthropogenic impact. *J. Environ. Monit.*, 13, 3399–3408.

Santos, S. A. O., Vilela, C., Freire, C. S. R., Abreu, M. H., Rocha, S. M., and Silvestre, A. J. D. (2015). Chlorophyta and Rhodophyta macroalgae: A source of health promoting phytochemicals. *Food Chem.*, 183, 122–128.

Santschi, P., Höhener, P., Benoit, G., and Buchholtzten Brink, M. (1990). Chemical processes at the sediment–water interface. *Mar. Chem.*, 30, 269–315.

Savage, C. (2005). Tracing the influence of sewage nitrogen in a coastal ecosystem using stable nitrogen isotopes. *Ambio*, 34, 145–150.

Schreyers, L., van Emmerik, T., Biermann, L., and Le Lay, Y.-F. (2021). Spotting green tides over Brittany from space: Three decades of monitoring with Landsat imagery. *Remote Sens.*, 13, article no. 1408.

Sigmon, D. E. and Cahoon, L. B. (1997). Comparative effects of benthic microalgae and phytoplankton on dissolved silica fluxes. *Aquat. Microb. Ecol.*, 13, 275–284.

Sloth, N. P., Blackburn, H., Hansen, L. S., Risgaard-Petersen, N., and Lomstein, B. Aa. (1995). Nitrogen cycling in sediments with different organic loading. *Mar. Ecol. Prog. Ser.*, 116, 163–170.

Ståhlberg, C., Bastviken, D., Svensson, B. H., and Rahm, L. (2006). Mineralisation of organic matter in coastal sediments at different frequency and duration of resuspension. *Estuar. Coast. Shelf Sci.*, 70, 317–325.

Volkman, J. K. (1986). A review of sterol markers for marine and terrigenous organic matter. *Org. Geochem.*, 9, 83–99.

Volkman, J. K., Rohjans, D., Rullkötter, J., Scholz-Böttcher, B. M., and Liebezeit, G. (2000). Sources and diagenesis of organic matter in tidal flat sediments from the German Wadden Sea. *Cont. Shelf Res.*, 20, 1139–1158.

Wang, P., Mi, W., Xie, Z., Tang, J., Apel, C., Joerss, H., Ebinghaus, R., and Zhang, Q. (2020). Overall

comparison and source identification of PAHs in the sediments of European Baltic and North Seas, Chinese Bohai and Yellow Seas. *Sci. Total Environ.*, 737, article no. 139535.

Watson, S. J., Cade-Menun, B. J., Needoba, J. A., and Peterson, T. D. (2018). Phosphorus forms in sediments of a river-dominated estuary. *Front. Mar. Sci.*, 5, article no. 302.

Welsh, D. T. (2003). It's a dirty job but someone has to do it: The role of marine benthic macrofauna in organic matter turnover and nutrient recycling to the water column. *Chem. Ecol.*, 19, 321–342.

Woolfenden, E. N. M., Hince, G., Powell, S. M., Stark,

S. C., Snape, I., Stark, J. S., and George, S. C. (2011). The rate of removal and the compositional changes of diesel in Antarctic marine sediment. *Sci. Total Environ.*, 410–411, 205–216.

Yan, B., Abrajano, T. A., Bopp, R. F., Chaky, D. A., Benedict, L. A., and Chillrud, S. N. (2005). Molecular tracers of saturated and polycyclic aromatic hydrocarbon inputs into Central Park Lake, New York City. *Environ. Sci. Technol.*, 39, 7012–7019.

Yunker, M. B., Macdonald, R. W., Vingarzan, R., Mitchell, R. H., Goyette, D., and Sylvestre, S. (2002). PAHs in the Fraser River basin: a critical appraisal of PAH ratios as indicators of PAH source and composition. *Org. Geochem.*, 33, 489–515.